



# Combined effect of radiation absorption and exponential parameter on chemically reactive Casson fluid over an exponentially stretching sheet

C. Arruna Nandhini<sup>a,\*</sup>, S. Jothimani<sup>a</sup>, Ali J. Chamkha<sup>b</sup>

<sup>a</sup> Department of Mathematics, Government Arts College (Autonomous), Coimbatore 641018, Tamil Nadu, India

<sup>b</sup> Faculty of Engineering, Kuwait College of Science and Technology, Doha District, 35004, Kuwait

## ARTICLE INFO

### Keywords:

Exponentially stretching sheet  
Viscous dissipation  
Chemical reaction  
Casson fluid  
Radiation absorption

## ABSTRACT

The essence of the current examination is to predict the consequence of the simultaneous incorporation of radiation absorption and chemical reaction on Casson fluid flow across an exponentially stretching surface under the influence of various exponential order flow parameters. The regulating partial differential equations are transitioned into ordinary differential equations by employing a best-suited similarity transformation. The resultant equations are computed numerically using MATLAB bvp4c built-in technique. In order to justify the precision of the numerical method used, the numerical values obtained in a constrained scenario are correlated with the outcomes existing in the literature. The impacts of multifarious dimensionless parameters on velocity profile, temperature and concentration distributions are illustrated graphically. The effect of involved parameters on skin friction coefficient, Nusselt number and Sherwood number are tabulated. The Combined influence of chemical reaction and radiation absorption with the incorporation of an exponential parameter on the flow field is trailblazing since the radiation absorption skyrockets the temperature, but on the contrary, chemical reaction decelerates the temperature.

## 1. Introduction

The preponderance of current research sheds light on the inquisition of flow across a stretching surface in which the velocity is presumed to be linearly proportional. Nevertheless, it is frequently asserted that the sheet need not inevitably be linear. This brainwave led innumerable researchers and scientists to probe into the fluid flow past an exponentially stretching surface. Magyari and Keller<sup>1</sup> initiated the inspection of similarity solution for the continuous exponentially stretching surface, which incorporates an exponential dependence on the temperature distribution, stretching velocity and also on the similarity variable with respect to the direction in which the stretching occurs. They procured the numerical solution as well as the analytical solution. Moreover, their proposed model was compared with the existing power-law model. Following the pioneering work of Magyari and Keller<sup>1</sup> and motivated by Gupta and Gupta,<sup>2</sup> Elbashbeshy<sup>3</sup> scrutinized the impact of suction across an exponentially stretching continuous sheet. Iteration algorithm was implemented by him to acquire the solution of the governing equations numerically. He concluded that suction enhances the coefficient of friction and heat transfer. In all the above-mentioned studies, the intractable impact of magnetic field was neglected. This motivated Al-Odat et al.<sup>4</sup> to investigate the flow in light of the magnetic field effects numerically. The significance of the

magnetic field and its modern applications were highlighted by Kataria and Mittal<sup>5</sup> and Shamshuddin et al.<sup>6</sup>

Sajid and Hayat<sup>7</sup> extended the evaluation of reference<sup>1</sup> by taking thermal radiation into account. Analytical solutions were elicited by the employment of Homotopy Analysis Method (HAM), which paved the way to conclude that the radiation parameter influences the thermal boundary layer thickness. Bidin and Nazar<sup>8</sup> numerically reinforced Sajid and Hayat's work using Keller box method. Numerical solution for the same problem together with magnetic field effect was sifted by Ishak.<sup>9</sup> His discussions stated that the transverse magnetic field opposed the transport phenomenon. Mandal and Mukhopadhyay<sup>10</sup> considered the similar problem but of exponential order. It is evident that enhancing the exponential parameter diminishes the velocity and temperature. Overwhelming applications of thermal radiation have prompted many authors to scrutinize the impact of thermal radiation on several types of fluid for different flow geometries recently (See Refs. 11–15). Combined influence of radiation and magnetic field past an oscillating vertical plate was modelled by Kataria and Mittal.<sup>16</sup> A recent study was carried out by Rahman et al.<sup>17</sup> past an exponentially stretching sheet by considering thermal radiation and heat source<sup>18</sup> or sink effects simultaneously. In addition to the previous works, exponential based heat source/sink effects were explored by Shamshuddin et al.<sup>19</sup>

\* Corresponding author.

E-mail addresses: [arruna98@gmail.com](mailto:arruna98@gmail.com) (C. Arruna Nandhini), [jothimanimaths@gacbe.ac.in](mailto:jothimanimaths@gacbe.ac.in) (S. Jothimani), [a.chamkha@kcst.edu.kw](mailto:a.chamkha@kcst.edu.kw) (A.J. Chamkha).

Not long ago, Rajput et al.<sup>20</sup> inspected the striking impact of buoyancy past an exponentially stretching sheet. From this study, it is obvious that, escalating the Eckert number skyrockets the temperature. Over an exponentially stretching sheet, Shamshuddin et al.<sup>21</sup> deduced that the temperature distribution markedly elevates with a rise in radiation parameter and Eckert number. Similarly, Shamshuddin et al.<sup>22</sup> noted that under different types of fluid and flow past an exponentially stretchable surface, the temperature distribution rises with an increase in the magnetic field parameter and Eckert number. Adding to the pre-existing literature, many authors like Kataria et al.<sup>23,24</sup> shed light on viscous dissipation under different geometries recently. Simultaneous heat and mass transfer play a major role since it is the core science of many industrial processes, especially in the domain of chemical engineering. In the immediate past, Reddy et al.<sup>25</sup> explored the impingement of chemical reaction across an exponentially stretching sheet. Numerical solutions were resolved via the Keller box technique, from which they surmised that higher values of chemical reaction parameter curtail the particle concentration. Recently, analytical work was carried out by Patel et al.<sup>26</sup> and Shamshuddin et al.<sup>27</sup> to study the effect of chemical reactions on different types of fluids. Moreover, it was justified by Shamshuddin et al.<sup>28</sup> that a weak rise in the wall friction and temperature gradient was noticed, but a significant rise was computed in the Sherwood number with an increase in the chemical reaction parameter.

Non-Newtonian fluids have been captivated by various researchers by virtue of their overwhelming practical applications. The Casson fluid<sup>29</sup> is a conspicuous one amidst many other non-Newtonian models. Mukhopadhyay et al.<sup>30</sup> examined the Casson fluid flow across a surface that stretches exponentially. The analytical solution in a constrained regime and numerical solution has been obtained via fourth order Runge–Kutta scheme. They concluded that a rise in the Casson parameter depletes the velocity but a reverse trend is observed in the temperature distribution. Extending,<sup>30</sup> Pramanik<sup>31</sup> stated that the temperature upswings with increasing radiation parameter in the case of Casson fluid flow. Similar to Ref. 31, presence of thermal radiation together with magnetic field effects was analysed numerically via shooting technique by Mukhopadhyay et al.<sup>32</sup> They concluded that magnetic parameter diminishes the transport rate. Of-late, Raju et al.<sup>33</sup> extended the exploration of Ref. 31 by considering the mass transfer of Casson fluid along an exponentially stretching sheet together with heat source and of exponential order. Numerical solutions were discussed by Raju et al.<sup>33</sup> for both Casson fluid and Newtonian fluid.

The existence of radiation absorption is, however, thought provoking, as the flow becomes much more complicated. In planetary atmosphere, absorption of radiation from adjoining stars is a paradigm of radiation absorption. Shercliff,<sup>34</sup> in his textbook, discussed the mass transfer of an electrically conducting viscous fluid along with radiation absorption. This is found to be efficacious in the domain of planetary research. Trailblazing examination of radiation absorption coupled with chemical reaction was carried out by Ibrahim et al.<sup>35</sup> Out of this, it was concluded that upliftment of absorption radiation parameter enhances the velocity and temperature profile. Following Ibrahim et al.,<sup>35</sup> Kumar et al.<sup>36</sup> employed Laplace transform technique to examine the impact of radiation absorption across an exponentially accelerated moving plate. Extension to micropolar fluid with radiation absorption for steady case was carried out by Narayana et al.<sup>37</sup> Both analytical and numerical solutions were presented by them and results analogous to Ref. 35 were justified. Under different geometry and Kuvshinski fluid under consideration, the influence of radiation absorption was solved using perturbation technique by Balamurugan et al.<sup>38</sup> Theoretically, Umamaheswar et al.<sup>39</sup> utilized similar technique of Balamurugan et al.<sup>38</sup> for Newtonian fluid. In such a case, it was stated that as the radiation absorption parameter rose, the friction factor and temperature distribution got enhanced. Governing equations were formulated by Reddy et al.<sup>40</sup> and scrutinized for unsteady hydromagnetic fluid flow with the addition of absorption of radiation and inferred that absorption

radiation parameter diminishes adjacent to the wall and skyrockets apart from the wall. In a constrained scenario, Ajibade and Umar's<sup>41</sup> work match with those of Ibrahim et al.,<sup>35</sup> which validates the essentiality of radiation absorption. A complimentary study to existing literature was accomplished by Sreedevi et al.,<sup>42</sup> which summarized that concentration escalates with augmenting radiation absorption. Not long ago, Reddy et al.<sup>43</sup> undertook the inquisition of Casson fluid with radiation absorption across a vertically oscillating plate. Finite difference scheme was employed, and indistinguishable conclusions to Ref. 35 were reckoned.

With these in mind, and as far as the authors are aware, there has never been a prior effort to evaluate the flow impact of Casson fluid along with radiation absorption and chemical reaction over an exponentially stretching sheet, which embodies an exponential dependence on the similarity variable, stretching velocity, temperature distribution, and concentration distribution. The novelty of the current analysis is the inspection of radiation absorption on Casson fluid flow past an exponentially stretching sheet under the influence of exponential order flow parameters as an extension to the work of Raju et al.<sup>33</sup> This furnishes the motivation for the current perusal where we effectuated similarity transformation to transfigure the partial differential equations (PDEs) that govern the flow into ordinary differential equations (ODEs). Numerical solutions were reckoned and the utilized MATLAB numerical technique was validated with the pre-existing literature. It is anticipated that the outcomes reported will supplement the previous studies and in addition yield vital information for practical applications in the near future.

## 2. Mathematical formulation

Taken into account is a viscous MHD Casson fluid past a surface that is exponentially stretching. Moreover, the Casson fluid is presumed to be incompressible and electrically conducting. By retaining the origin  $O$  fixed, the wall is stretched out about the  $x$ -axis. Likewise,  $y$ -axis is held perpendicular to the  $x$ -axis. The surface under consideration is inferred to coincide with  $y = 0$ . Additionally, the dynamics of the fluid is constrained to  $y > 0$ . In the transverse direction to the surface flow, under exertion is the magnetic field  $B(x) = B_0 e^{Nx/2L}$ , where  $B_0$  is a constant,  $N$  is the exponential parameter and  $L$  is the characteristic length. The aforesaid hypotheses are distinctly portrayed in Fig. 1.

“The rheological equation of state for an isotropic and incompressible flow of a Casson fluid is as follows

$$\tau_{ij} = \begin{cases} 2 \left( \mu_B + \frac{p_y}{\sqrt{2\pi}} \right) e_{ij}, & \pi > \pi_c \\ 2 \left( \mu_B + \frac{p_y}{\sqrt{2\pi_c}} \right) e_{ij}, & \pi < \pi_c \end{cases} \quad (2.1)$$

Here,  $\pi = e_{ij}e_{ij}$  and  $e_{ij}$  are the  $(i,j)$ th component of the deformation rate,  $\pi$  is the product of the component of deformation rate with itself,  $\pi_c$  is the critical value of this product based on non-Newtonian model,  $\mu_B$  is the plastic dynamic viscosity of the non-Newtonian fluid and  $p_y$  is the yield stress of the fluid”.<sup>13</sup>

For the case of Casson fluid, we considered  $\pi > \pi_c$  and  $p_y = \frac{\mu_B \sqrt{2\pi}}{\beta}$ , it is possible to say that the dynamic viscosity

$$\mu = \mu_B + \frac{p_y}{\sqrt{2\pi}} \quad (2.2)$$

Substituting the value of  $p_y$  in (2.2), we get

$$\mu = \mu_B \left( 1 + \frac{1}{\beta} \right) \quad (2.3)$$

The governing equations corresponding to the framework under deliberation by extending the work of Raju et al.<sup>33</sup> is formulated as:

$$\frac{\partial u}{\partial x} + \frac{\partial v}{\partial y} = 0 \quad (2.4)$$

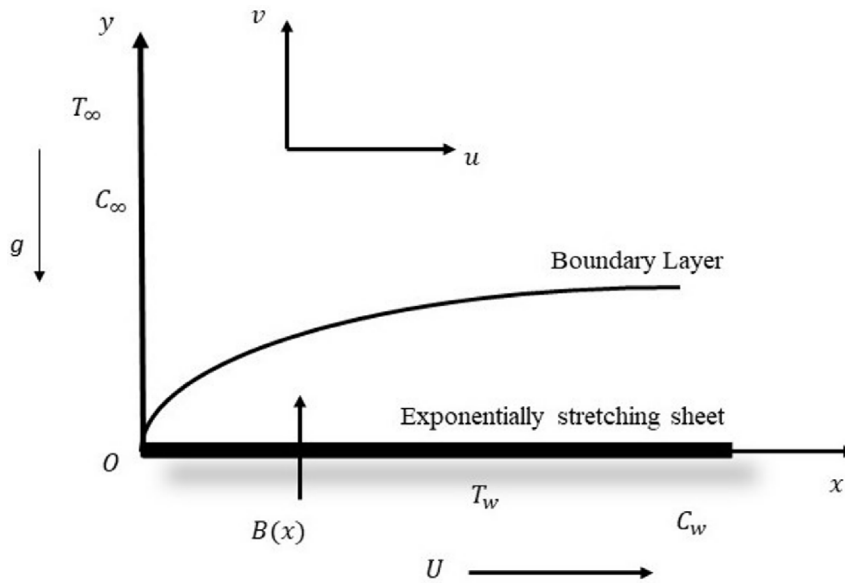


Fig. 1. Schematic representation of the fluid flow problem.

$$u \frac{\partial u}{\partial x} + v \frac{\partial u}{\partial y} = \nu \left( 1 + \frac{1}{\beta} \right) \frac{\partial^2 u}{\partial y^2} + g\beta_T (T - T_\infty) + g\beta_C (C - C_\infty) - \frac{\sigma B^2 u}{\rho} \quad (2.5)$$

$$\rho c_p \left( u \frac{\partial T}{\partial x} + v \frac{\partial T}{\partial y} \right) = \kappa \frac{\partial^2 T}{\partial y^2} - \frac{\partial q_r}{\partial y} + \mu_B \left( 1 + \frac{1}{\beta} \right) \left( \frac{\partial u}{\partial y} \right)^2 + Q (T - T_\infty) + Q^* (C - C_\infty) \quad (2.6)$$

$$u \frac{\partial C}{\partial x} + v \frac{\partial C}{\partial y} = D_m \frac{\partial^2 C}{\partial y^2} - k_l (C - C_\infty) \quad (2.7)$$

where  $u$  and  $v$  are the velocity components in the  $x$  and  $y$  directions respectively.  $\nu$  is the kinematic viscosity. Casson fluid parameter is  $\beta = \frac{\mu_B \sqrt{2\pi_c}}{\rho \nu}$ .  $g$  is the acceleration due to gravity.  $\beta_T$  and  $\beta_C$  are the thermal and concentration expansion coefficient respectively.  $T$ ,  $C$ ,  $T_\infty$  and  $C_\infty$  are the fluid temperature, fluid concentration, ambient fluid temperature and ambient fluid concentration respectively.  $\sigma$  is the electrical conductivity,  $\rho$  is the density,  $\rho c_p$  is the heat capacitance,  $\kappa$  is the thermal conductivity and  $D_m$  is the coefficient of mass diffusivity. Heat source/sink is  $Q = Q_0 e^{Nx/L}$ , chemical reaction is  $k_l = k_0 e^{Nx/L}$  and radiation absorption is  $Q^* = Q_0^* e^{Nx/L}$ .

Utilizing Rosseland approximation<sup>44</sup> for thermal radiation, radiative heat flux  $q_r$  can be written as follows:

$$q_r = -\frac{4\sigma^*}{3k^*} \frac{\partial T^4}{\partial y} \quad (2.8)$$

Here,  $\sigma^*$  is the Stefan-Boltzmann constant and  $k^*$  is the absorption coefficient.

“Assuming that the temperature difference within the flow is such that  $T^4$  may be expanded in a Taylor series and expanding  $T^4$  about  $T_\infty$  and neglecting higher orders, we get  $T^4 \equiv 4T_\infty^3 T - 3T_\infty^4$ ”.<sup>31</sup> And for that reason, Eq. (2.4) becomes:

$$\rho c_p \left( u \frac{\partial T}{\partial x} + v \frac{\partial T}{\partial y} \right) = \kappa \left( 1 + \frac{16\sigma^* T_\infty^3}{\kappa k^*} \right) \frac{\partial^2 T}{\partial y^2} + \mu_B \left( 1 + \frac{1}{\beta} \right) \left( \frac{\partial u}{\partial y} \right)^2 + Q (T - T_\infty) + Q^* (C - C_\infty) \quad (2.9)$$

### 3. Boundary conditions

The pertinent boundary constraints are enunciated as:

$$\text{at } y = 0 \quad u = U, \quad v = -V(x), \quad T = T_w, \quad C = C_w \quad (3.1)$$

$$\text{as } y \rightarrow \infty \quad u \rightarrow 0, \quad T \rightarrow T_\infty, \quad C \rightarrow C_\infty \quad (3.2)$$

At this juncture, stretching velocity  $U = U_0 e^{Nx/L}$ , surface temperature  $T_w = T_\infty + T_0 e^{Nx/2L}$  and surface concentration  $C_w = C_\infty + C_0 e^{Nx/2L}$ .  $U_0, T_0$  and  $C_0$  are the reference velocity, reference temperature and reference concentration respectively.  $V(x) = V_0 e^{Nx/2L}$ , “a special type of velocity at the wall is considered where  $V_0$  is a constant,  $V(x) > 0$  is the velocity of suction and  $V(x) < 0$  is the velocity of blowing”.<sup>31</sup>

### 4. Solution technique

As mentioned by Magyari and Keller,<sup>1</sup> it is not very surprising that in the current content there occurs a well-known similarity solution corresponding to the present problem. In this concern, with  $\eta$  as the similarity variable, the following similarity transformation is introduced:

$$\eta = \sqrt{\frac{U_0}{2\nu L}} e^{Nx/2L} y \quad (4.1)$$

$$u = U_0 e^{Nx/L} f'(\eta) \quad (4.2)$$

$$v = -\sqrt{\frac{\nu U_0}{2L}} e^{Nx/2L} N \{ f(\eta) + \eta f'(\eta) \} \quad (4.3)$$

$$T = T_\infty + T_0 e^{Nx/2L} \theta(\eta) \quad (4.4)$$

$$C = C_\infty + C_0 e^{Nx/2L} \varphi(\eta) \quad (4.5)$$

Upon substitution of Eqs. (4.1)–(4.5) in Eqs. (2.5), (2.9) and (2.7), the governing equations transmuted to the coupled ODEs of the form:

$$\left( 1 + \frac{1}{\beta} \right) f'''' + N (f f'' - 2f'^2) + 2Gr\theta + 2Gc\varphi - M f' = 0 \quad (4.6)$$

$$\frac{1}{Pr} \left( 1 + \frac{4}{3} R \right) \theta'' - N (f' \theta - f \theta') + Ec \left( 1 + \frac{1}{\beta} \right) (f'')^2 + Q_H \theta + R_c \varphi = 0 \quad (4.7)$$

$$\varphi'' - N.Sc (f' \varphi - f \varphi') - k.Sc \varphi = 0 \quad (4.8)$$

Similarly, the employment of (4.1)–(4.5) in Eqs. (3.1) and (3.2) produce:

$$f'(\eta) = 1, \quad f(\eta) = S, \quad \theta(\eta) = 1 \text{ and } \varphi(\eta) = 1 \quad \text{at } \eta = 0. \quad (4.9)$$

$$f'(\eta) \rightarrow 0, \quad \theta(\eta) \rightarrow 0 \text{ and } \varphi(\eta) \rightarrow 0 \quad \text{as } \eta \rightarrow \infty. \quad (4.10)$$

Here, prime notation points to  $\eta$ -dependent differentiation.

Several non-dimensional parameters obtained after transmutation are as follows: Magnetic field parameter  $M = \frac{2L\sigma B_0^2}{\rho U_0}$ , Thermal

Grashof number  $Gr = \frac{gL\beta_T(T_w - T_\infty)}{U^2}$ , Solutal Grashof number  $Gc = \frac{gL\beta_C(C_w - C_\infty)}{U^2}$ , Prandtl number  $Pr = \frac{\nu}{\alpha}$  where  $\alpha$  is the thermal diffusivity, Radiation parameter  $R = \frac{4\sigma^*T_\infty^3}{\kappa k^*}$ , Eckert number  $Ec = \frac{U^2}{c_p(T_w - T_\infty)}$ , Heat source/sink  $Q_H = \frac{2Q_0L}{U_0\rho c_p}$ , Radiation absorption parameter  $R_a = \frac{2Q_0^*C_0L}{U_0T_0\rho c_p}$ , Schmidt number  $Sc = \frac{\nu}{D_m}$ , Chemical reaction parameter  $k = \frac{k_0L}{U_0}$  and suction/injection  $S = \frac{v_0}{\sqrt{\frac{\nu U_0}{2L}}}$ .

The interest-generating physical quantities, namely skin-friction coefficient  $C_f$ , Nusselt Number  $Nu_x$  and Sherwood number  $Sh_x$  are procured as follows:

$$\frac{C_f \sqrt{Re_x/2}}{\sqrt{x/L}} = \left(1 + \frac{1}{\beta}\right) f''(0)$$

$$\frac{Nu_x}{\sqrt{Re_x/2} \sqrt{x/L}} = -\theta'(0)$$

$$\frac{Sh_x}{\sqrt{Re_x/2} \sqrt{x/L}} = -\phi'(0)$$

where  $Re_x = Ux/\nu$  is the Reynolds number.

### 5. Numerical procedure

MATLAB furnishes a platform to resolve the boundary value problems (BVPs). The transmogrified equations (4.6)–(4.10) are solved numerically by employing the MATLAB package bvp4c.<sup>45</sup> bvp4c is a finite difference algorithm that incorporates the three-stage Lobatto IIIa collocation formula.<sup>46</sup> bvp4c can be effectuated by altering the BVP as an initial value problem (IVP). By utilizing the linearity technique<sup>47</sup> such as (see Ref. 48)

$$“y_1 = f, y_2 = f', y_3 = f'', y_4 = \theta, y_5 = \theta', y_6 = \varphi \text{ and } y_7 = \varphi'.”$$

Eqs. (4.6) to (4.10) emerge as simultaneous first-order ODEs as follows:

$$y_3' = \frac{1}{\left(1 + \frac{1}{\beta}\right)} [-N(y_1y_3 - 2y_2y_2) - 2Gr y_4 - 2Gc y_6 + M y_2],$$

$$y_5' = \frac{Pr}{\left(1 + \frac{4}{3}R\right)} \left[ N(y_2y_4 - y_1y_5) - Ec \left(1 + \frac{1}{\beta}\right) y_3y_3 - Q_H y_4 - R_a y_6 \right]$$

and

$$y_7' = NSc(y_2y_6 - y_1y_7) + kScy_6,$$

with the boundary conditions

$$y_1(0) = S, y_2(0) = 1, y_4(0) = 1, y_6(0) = 1, y_2(\infty) \rightarrow 0, y_4(\infty) \rightarrow 0 \text{ and } y_6(\infty) \rightarrow 0.$$

The values are calculated at the far field boundary condition  $\eta_\infty = \eta_{max}$  ( $= 10$ ).

### 6. Results and discussion

#### 6.1. Justification of the numerical findings

In order to validate the precision of the numerical method used, the values of  $f''(0)$  and  $[-\theta'(0)]$  evaluated for Newtonian fluid (for special cases) are compared with the prior findings that have been published in the literature. In the absence of mass transfer, magnetic field, heat source/sink, radiation absorption, buoyancy effects, viscous dissipation and suction/injection, and for the case in which the exponential parameter is of unity, the values obtained match with those of Mukhopadhyay et al.,<sup>32</sup> Pramanik,<sup>31</sup> Bidin and Nazar,<sup>8</sup> Elbashbeshy<sup>3</sup> and Magyari and Keller<sup>1</sup> (See Tables 1 and 2).

The quantities  $C_f$ ,  $Nu_x$  and  $Sh_x$  pin hopes on  $\left(1 + \frac{1}{\beta}\right) f''(0)$ ,  $-\theta'(0)$  and  $-\phi'(0)$ . From Table 3, it is obvious that  $C_f$ ,  $Nu_x$  and  $Sh_x$  diminish

**Table 1**  
Correlation of  $f''(0)$  under special case and for Newtonian fluid.

Magyari and Keller <sup>1</sup>	Elbashbeshy <sup>3</sup>	Bidin and Nazar <sup>8</sup>	Mukhopadhyay et al. <sup>32</sup>	Present study
-1.28180	-1.28181	-1.28180	-1.28182	-1.28182

**Table 2**  
Correlation of  $[-\theta'(0)]$  for variation in  $Pr$  and  $R$ , and for Newtonian fluid.

$Pr$	$R$	Bidin and Nazar <sup>8</sup>	Pramanik <sup>31</sup>	Mukhopadhyay et al. <sup>32</sup>	Present study with $N = 1$
1	0	0.9547	0.9547	0.9547	0.9548
2		1.4714	1.4714	1.4714	1.4715
3		1.8691	1.8691	1.8691	1.8691
5			2.5001	2.5001	2.5001
10			3.6603	3.6603	3.6603
1	0.5	0.6765	0.6765		0.6767
	1	0.5315	0.5315		0.5313
2	0.5	1.0735	1.0734		1.0735
	1	0.8627	0.8626		0.8629
3	0.5	1.3807	1.3807		1.3807
	1	1.1214	1.1213		1.1214

with enhancement of  $M$  and rises with an upliftment in the values of  $Gr$  and  $Gc$ . Enhancement of  $R$ ,  $Ec$  and  $R_a$  depreciates  $Nu_x$  and skyrockets  $C_f$  and  $Sh_x$ . A rise in the values of  $k$  and  $N$  declines  $C_f$  but augments  $Nu_x$  and  $Sh_x$ . Increasing  $Q_H$  suppresses  $C_f$  and  $Sh_x$  whereas reverse trend is perceived in the case of  $Nu_x$ .

#### 6.2. Impact of multifarious apposite parameters on $f'(\eta)$ , $\theta(\eta)$ and $\phi(\eta)$

In order to keep things brief, the illustrations through figures are propounded for the influence of several pertaining parameters on velocity profile  $f'(\eta)$ , temperature distribution  $\theta(\eta)$  and concentration distribution  $\phi(\eta)$ . The values  $Ec = 0.01$ ,  $M = 0.5$ ,  $R_a = 0.5$ ,  $Gr = Gc = 1$ ,  $Pr = 0.71$ ,  $Sc = 0.6$ ,  $S = 0.5$ ,  $N = 0.5$ ,  $R = 0.3$ ,  $Q_H = 0.4$ ,  $\beta = 0.5$  and  $k = 0.1$  are treated as fixed for numerical results, all through this inspection, with the exception that the varied values are mentioned explicitly in corresponding figures.

Fig. 2 depicts the dominance of  $M$  on  $f'(\eta)$ . For  $N = 1$ , enhancement of  $M$  depreciates  $f'(\eta)$ . The transport rate is notably dwindling as a consequence of the transverse magnetic field, which instigates drag. This drag is induced in terms of Lorentz force. Moreover, Lorentz force skyrockets as  $M$  augments, which in-turn resists the flow to a greater extent. Moreover, escalating  $M$ , proliferates the thermal and solutal boundary layer thickness. On the grounds of this,  $\theta(\eta)$  and  $\phi(\eta)$  gets soared as  $M$  rises. This is seen vividly in Figs. 3 and 4 respectively.

Fig. 5 illustrates the impact of incorporating thermal radiation. It is obvious from the figure that an intensification of  $R$  augments  $\theta(\eta)$ . Incorporating thermal radiation into a flow model does, in fact, amplify the fluid flow's temperature domain. This is attributable to the enlargement of  $\kappa$  in a fluid that conducts electricity. Moreover, this is in agreement with the physical fact that the thermal boundary layer thickness increases with increasing  $R$ . Thermal radiation enhances the effective thermal diffusivity and thus the temperature increases.

The effect of exponential parameter has been depicted in Figs. 6–8. In  $f'(\eta)$ , for smaller values of  $N$ , the trend increases suddenly and, at some point, starts to decrease gradually. But this is not the case for larger values of  $N$ . Contrariwise, for both larger and smaller values of  $N$ , the trend tends to decline. As  $N$  rises,  $f'(\eta)$ ,  $\theta(\eta)$  and  $\phi(\eta)$  declines. Since the flow parameters are of exponential order, the value of  $N$  has a noticeable impact on the velocity field, temperature distribution and concentration distribution. Both for smaller and larger values of  $N$ , the novel results are procured.

The conversion of species takes place as a result of chemical reactions. Fig. 9 depicts the repercussions of encompassing  $k$  in the equation regulating the mass transfer. The curve rises in the neighbourhood of the wall and suddenly decreases far away from the wall. Further it is

**Table 3**  
 Tabulation of numerical values of  $\left(1 + \frac{1}{\beta}\right) f''(0)$ ,  $-\theta'(0)$  and  $-\phi'(0)$  for Casson fluid and for fixed values  $Pr = 0.7$ ,  $Sc = 0.6$  and  $S = 0.5$ .

$M$	$R$	$N$	$k$	$Q_H$	$Ec$	$R_o$	$Gr$	$Gc$	$\left(1 + \frac{1}{\beta}\right) f''(0)$	$-\theta'(0)$	$-\phi'(0)$
0.5	0.3	1	0.1	0.4	0.01	0.5	1	1	-2.15093	1.51960	1.88878
0.8									-2.39913	1.50956	1.87934
1.2									-2.70901	1.49698	1.86753
0.5	0.5								-2.08778	1.38133	1.89157
	0.8								-2.00546	1.22846	1.89527
	0.3	2							-4.06909	2.21543	2.75070
		3							-5.49492	2.78490	3.46661
		0.5	0.3						-2.16559	1.52072	1.93097
			0.5						-2.17925	1.52178	1.97204
			0.1	0.6					-2.17228	1.57026	1.88784
				0.8					-2.19174	1.61912	1.88700
				0.4	0.05				-2.14197	1.50801	1.88920
					0.1				-2.13085	1.49371	1.88973
					0.01				-2.13498	1.47448	1.88945
						0.7			-2.11913	1.42942	1.89012
						0.9			-2.11913	1.42942	1.89012
						0.5	3		-0.47057	1.56408	1.93364
							5		1.10905	1.60084	1.97172
							1	3	-0.70275	1.55479	1.92468
								5	0.67996	1.58520	1.95634

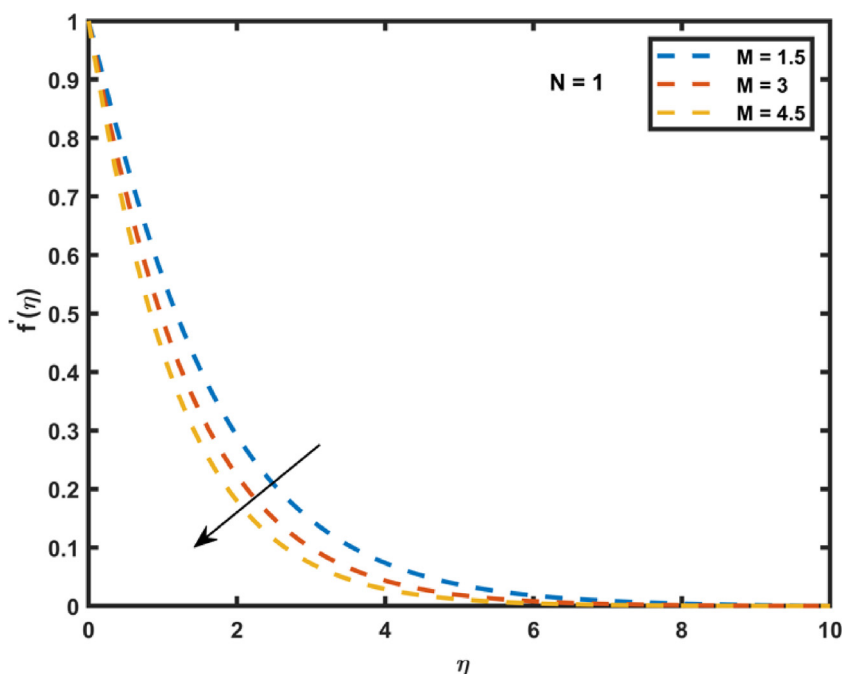


Fig. 2. Velocity profile for various  $M$ .

noted that for larger values of  $\beta$ , as  $k$  increases,  $f'(\eta)$  subsides. For negligible values of  $N$ , the influence of  $k$  on  $\theta(\eta)$  and  $\phi(\eta)$  are depicted in Figs. 10–11. It is seen vividly that  $\theta(\eta)$  and  $\phi(\eta)$  declines as  $k$  gets magnified. Since every flow parameter has an exponential dependence on the flow field, the simultaneous effect of the exponential parameter and the chemical reaction parameter is significant.

Figs. 12 and 13 disclosed the significant effect of  $Q_H$  on  $f'(\eta)$  and  $\theta(\eta)$  respectively. For larger values of  $\beta$ , enhancing  $Q_H$  decreases  $f'(\eta)$  as well as  $\theta(\eta)$ . Additionally, it demonstrated that temperature enhancement takes place when heat is produced. Moreover, this variation is predicted to be caused by declination of fluid’s thermal and kinetic energy. It is expected that the increase in the heat source parameter releases the heat energy to the flow, which causes enhancement of temperature distribution. But the dominance of external heat produces a reverse trend, contrary to the expected outcome.

The Eckert number provides a measure of the kinetic energy of the flow relative to the enthalpy difference across the thermal boundary layer. It is used to characterize heat dissipation in high-speed flows for which viscous dissipation is significant. From Fig. 14, it is evident that  $\theta(\eta)$  skyrockets as  $Ec$  augments. This occurs due to frictional heating in the fluid which causes heat to be generated as  $Ec$  increases. Consequently, an upsurge in  $Ec$  leads to work being done against the stresses of the viscous fluid, which transmutes kinetic energy into internal energy. Also, Eckert number signifies the quantity of mechanical energy converted via internal friction to thermal energy i.e., heat dissipation. This indirectly emphasizes the vitality of viscous dissipation in the energy equation.

Figs. 15 and 16 portrays the effect  $\beta$  on  $f'(\eta)$  and  $\theta(\eta)$  respectively. It is perceived from Fig. 15 that as  $\beta$  increases,  $f'(\eta)$  decreases. As  $\beta$  increases, the yield stress  $p_y$  falls, and consequently, the velocity

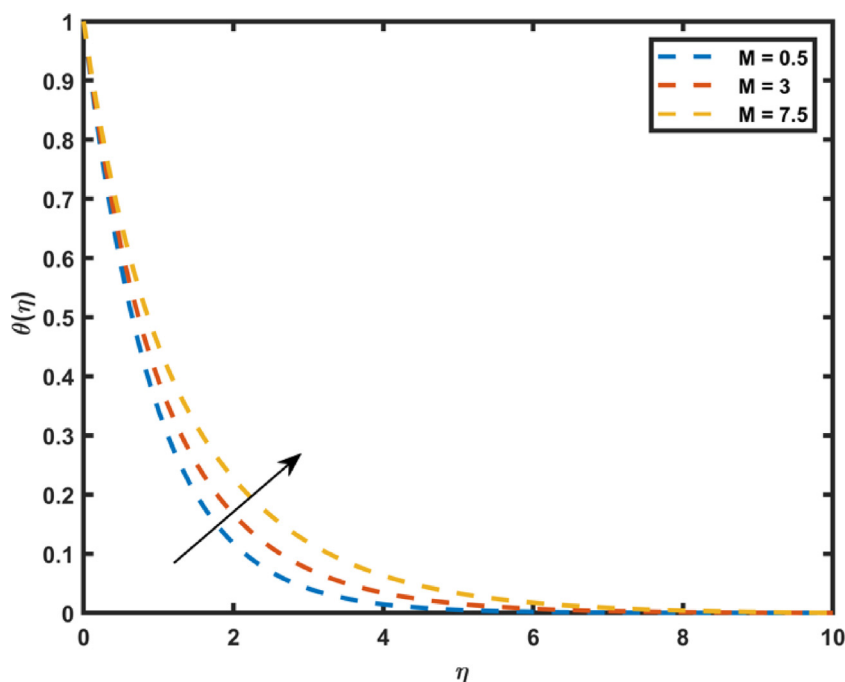


Fig. 3. Temperature distribution for various  $M$ .

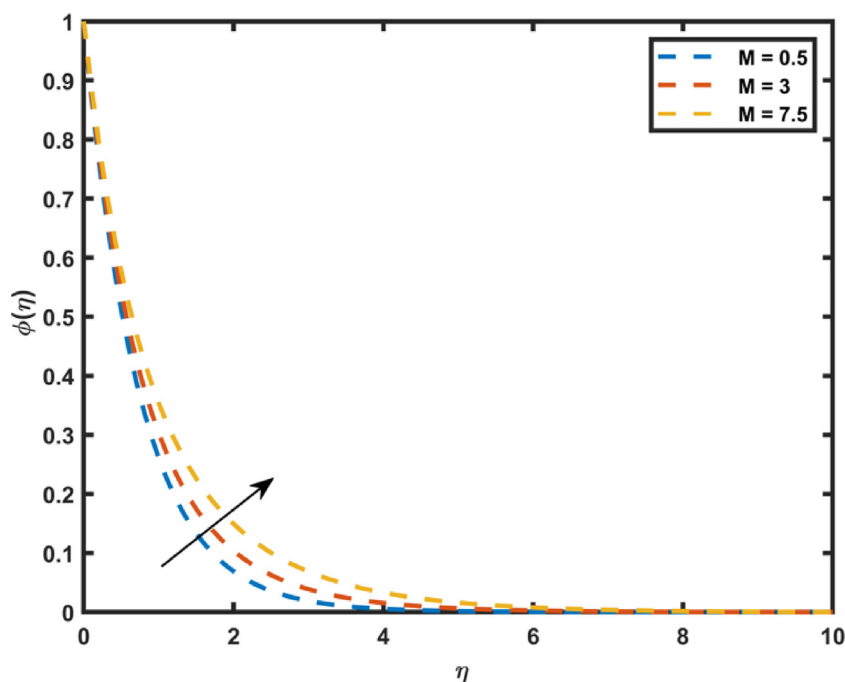


Fig. 4. Concentration distribution for various  $M$ .

boundary layer thickness decreases. But on the contrary, for  $N = 1$ , as  $\beta$  enhances,  $\theta(\eta)$  proliferates. A rise in  $\beta$  actually resists the flow of the fluid since it drastically reduces  $p_y$  of the Casson fluid and raises  $\mu_B$ . This resistance is accountable for the escalation of temperature as well. It is important to note that the higher value of  $\beta$  leads to Newtonian fluid.

Absorption of electromagnetic radiation transforms electromagnetic energy into internal energy. This transformation generates heat, which

in turn escalates the temperature distribution. Distinguishing the consequences of  $R_a$  for Prandtl number  $Pr = 6.83$  (methanol) and  $Pr = 0.7$  (air) is noted in Fig. 17. In the case of higher  $Pr$ , i.e., for methanol (in this case), the curve slightly rises close to the wall and diminishes smoothly apart from the wall. But this is not the trend for smaller  $Pr$ , i.e., air (in this case). Thus, as  $R_a$  boosts up,  $\theta(\eta)$  increases. This clearly shows that absorption of radiation is a significant phenomenon, which has a striking effect on the temperature distribution.

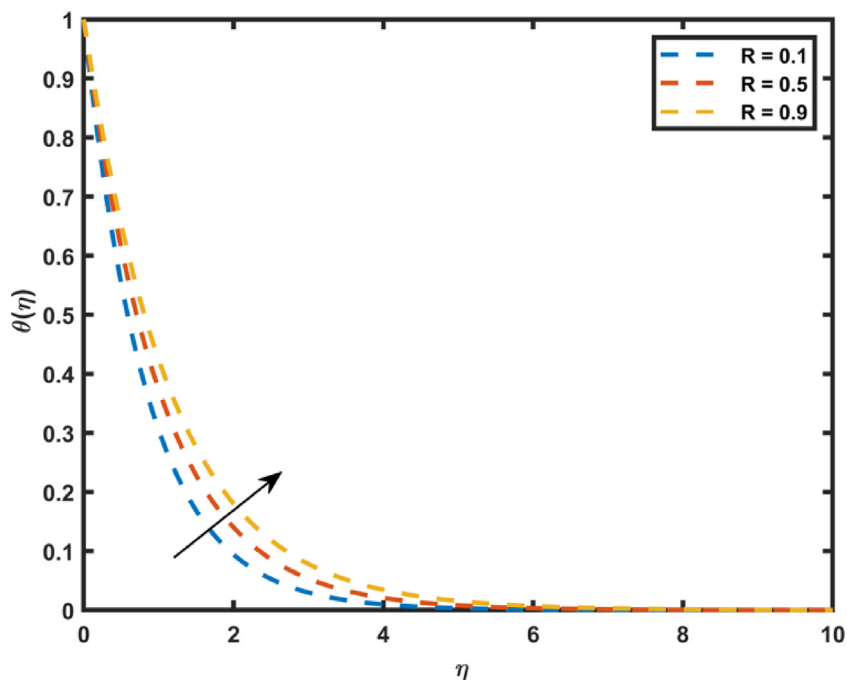


Fig. 5. Temperature distribution for various  $R$ .

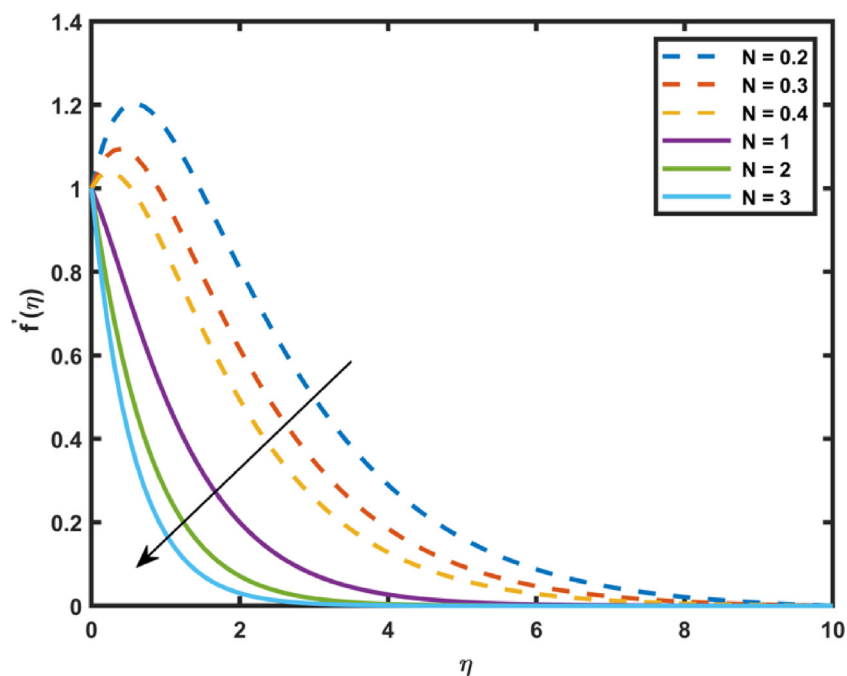


Fig. 6. Velocity profile for various  $N$ .

### 7. Conclusions

The outcomes of this study can be briefly summarized as follows:

- The effect of  $k$  suppresses  $\theta(\eta)$  and  $\phi(\eta)$  which in turn causes the enhancement of  $Nu_x$  and  $Sh_x$ .
- An upsurge in the values of  $Q_H$  and  $N$  augments the heat transfer rate and tends to curtail the friction factor.
- The increasing effect of  $M$  increases  $\theta(\eta)$  and  $\phi(\eta)$ .
- It is intriguing to note that the effect of  $N$  is so influencing and depreciates the velocity field.

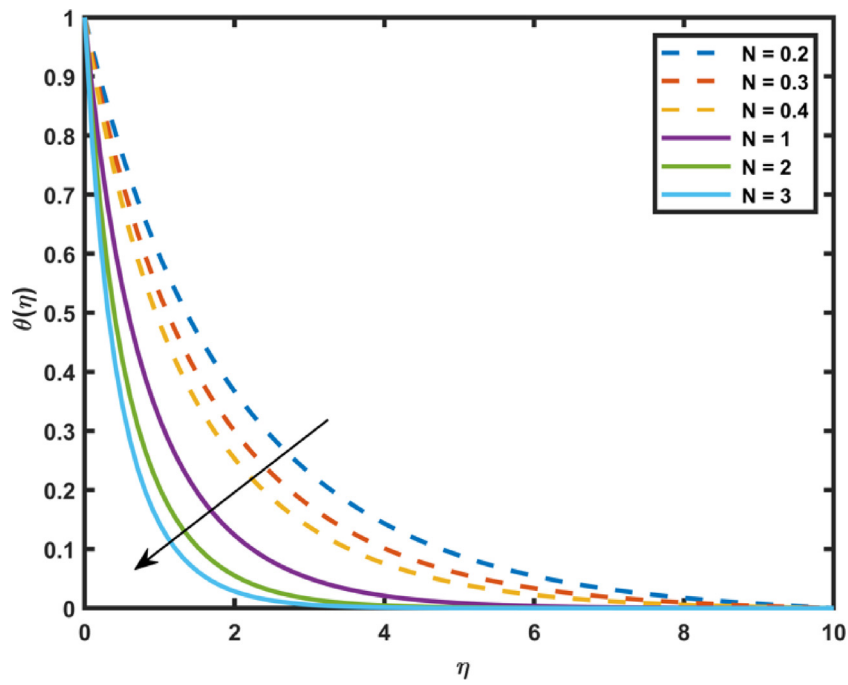


Fig. 7. Temperature distribution for various  $N$ .

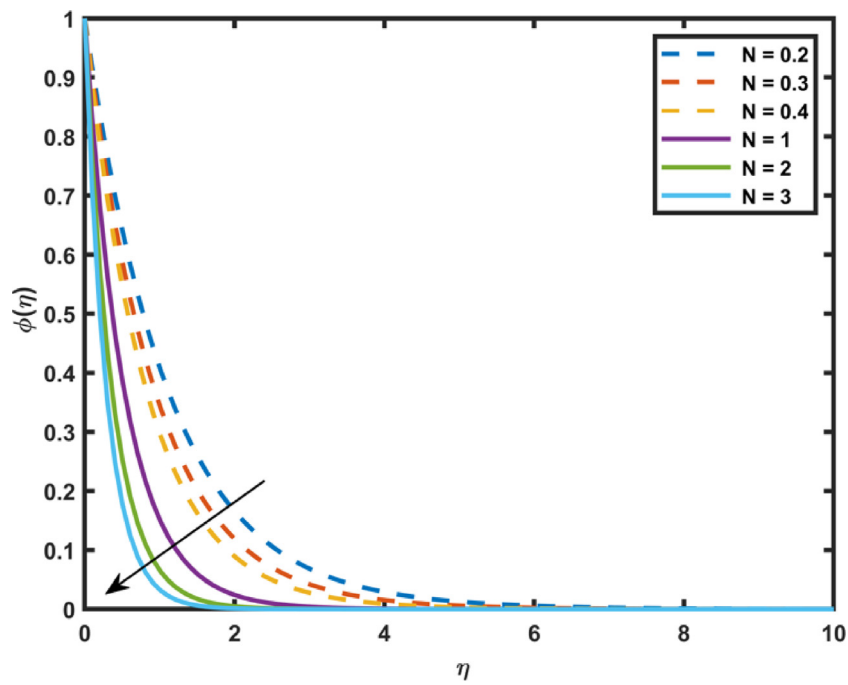


Fig. 8. Concentration distribution for various  $N$ .

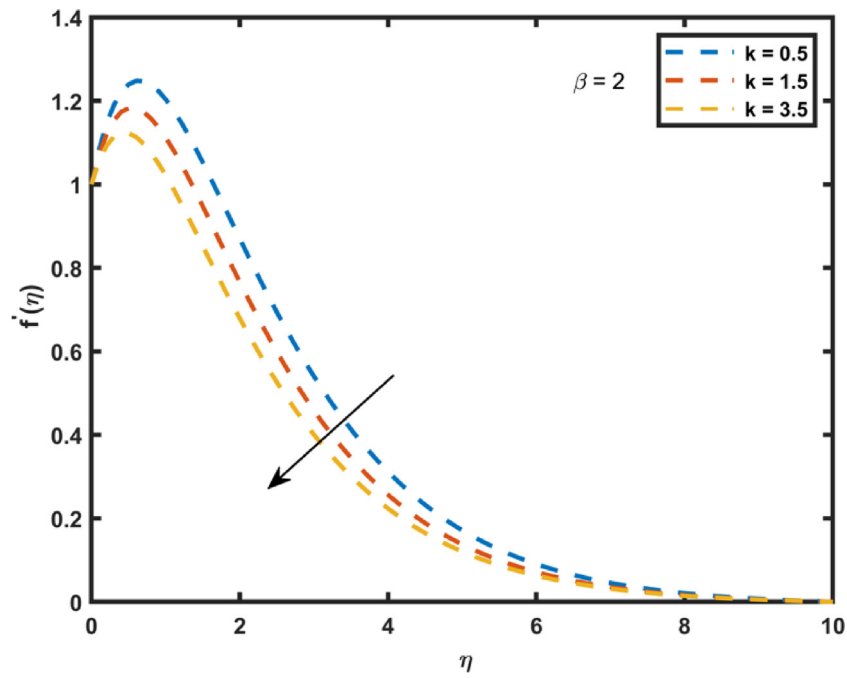


Fig. 9. Velocity profile for various  $k$ .

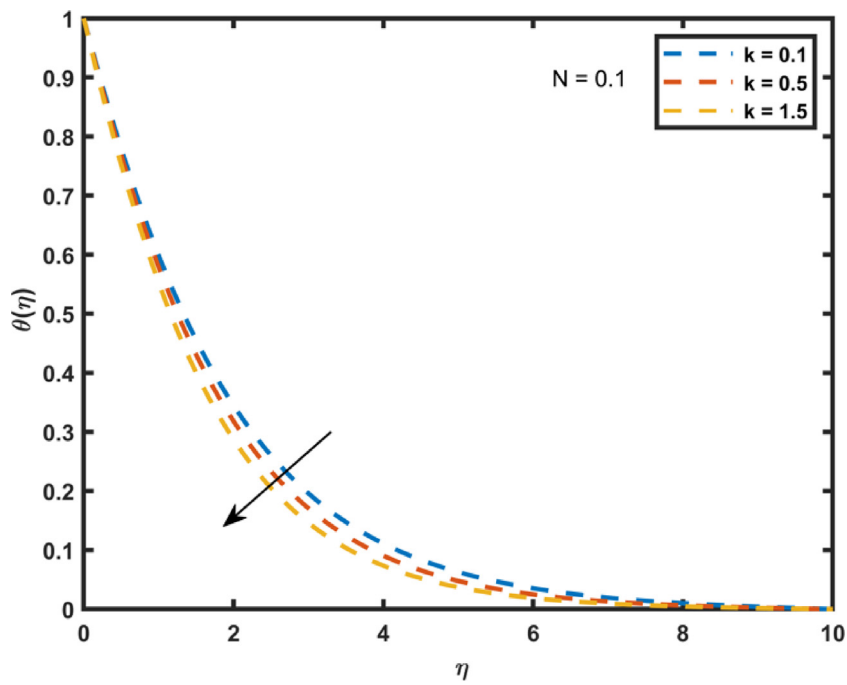


Fig. 10. Temperature distribution for various  $k$ .

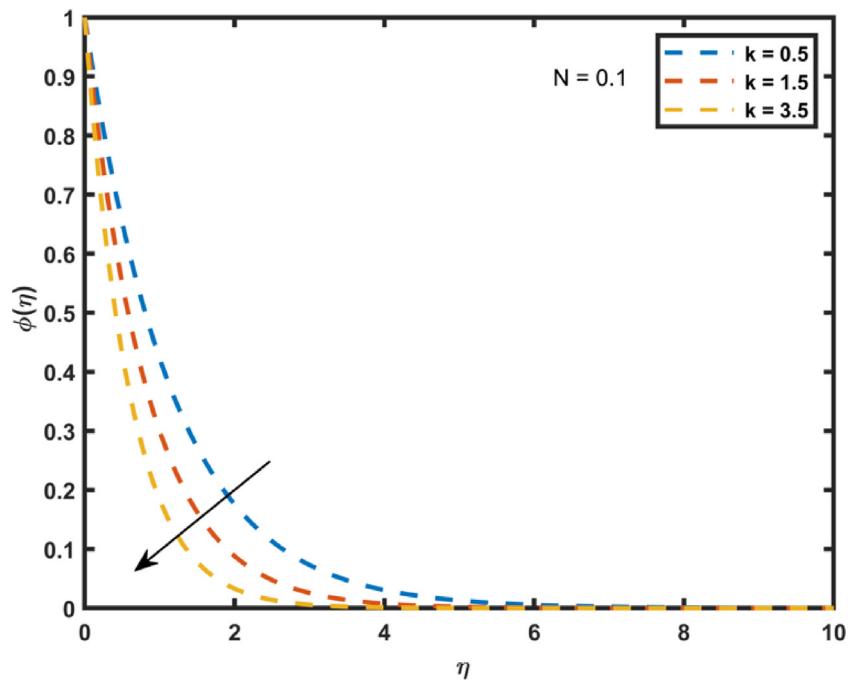


Fig. 11. Concentration distribution for various  $k$ .

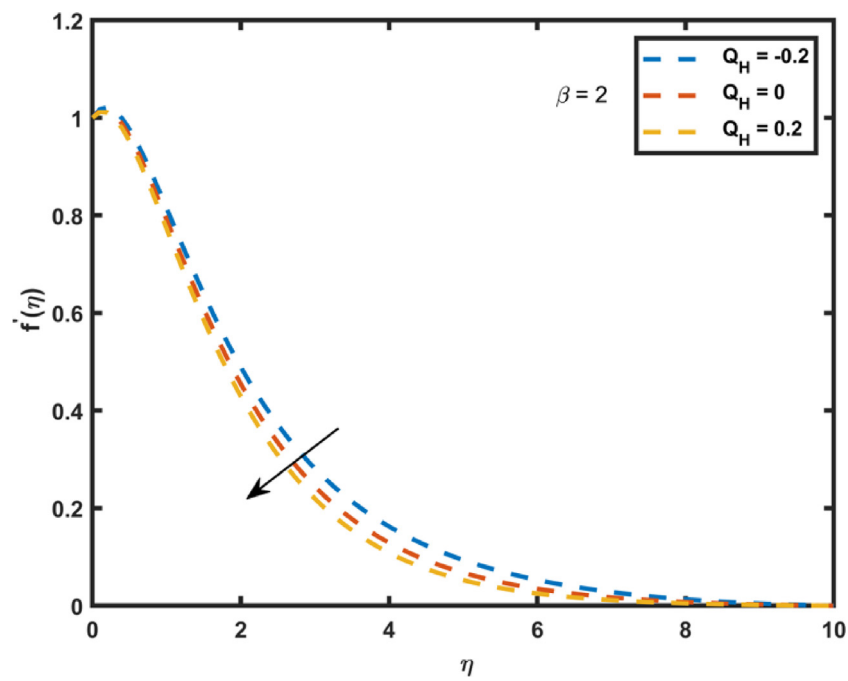


Fig. 12. Velocity profile for various  $Q_H$ .

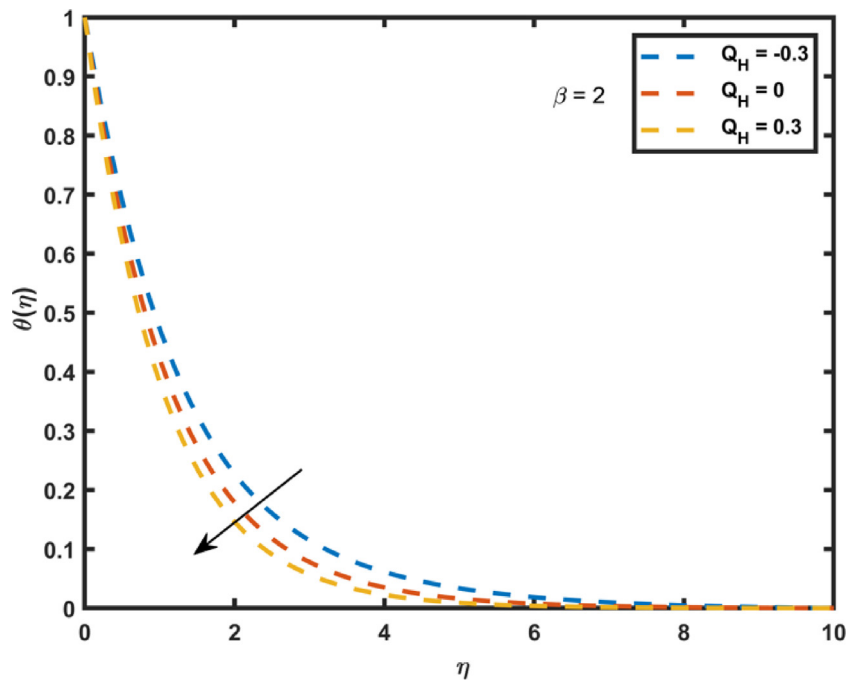


Fig. 13. Temperature distribution for various  $Q_H$ .

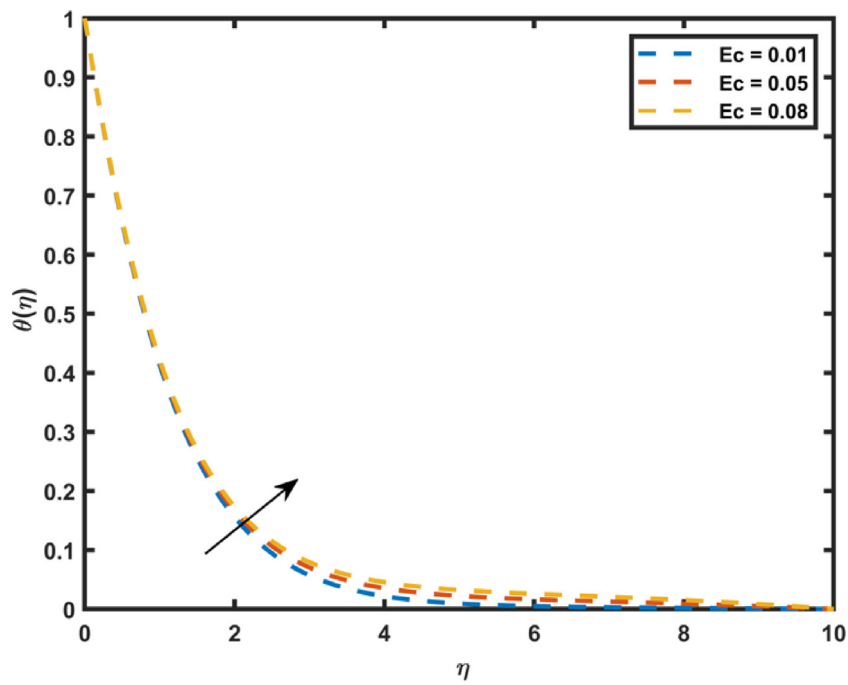


Fig. 14. Temperature distribution for various  $Ec$ .

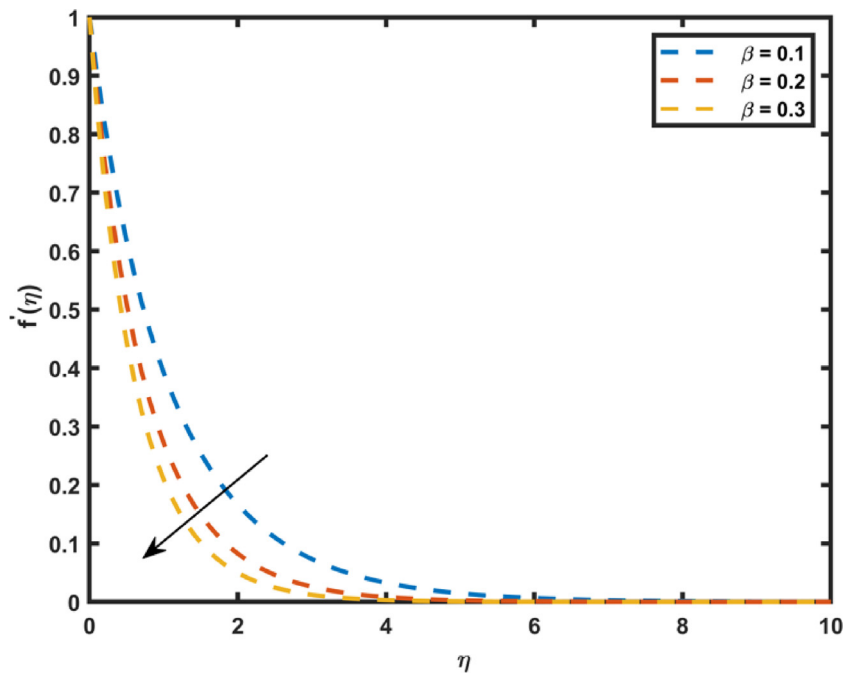


Fig. 15. Velocity profile for various  $\beta$ .

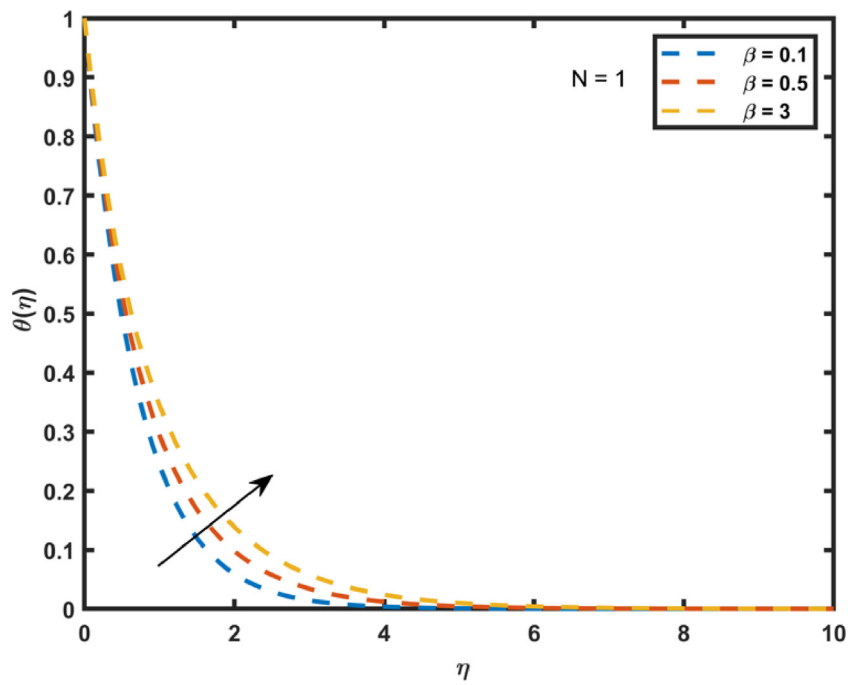


Fig. 16. Temperature distribution for various  $\beta$ .

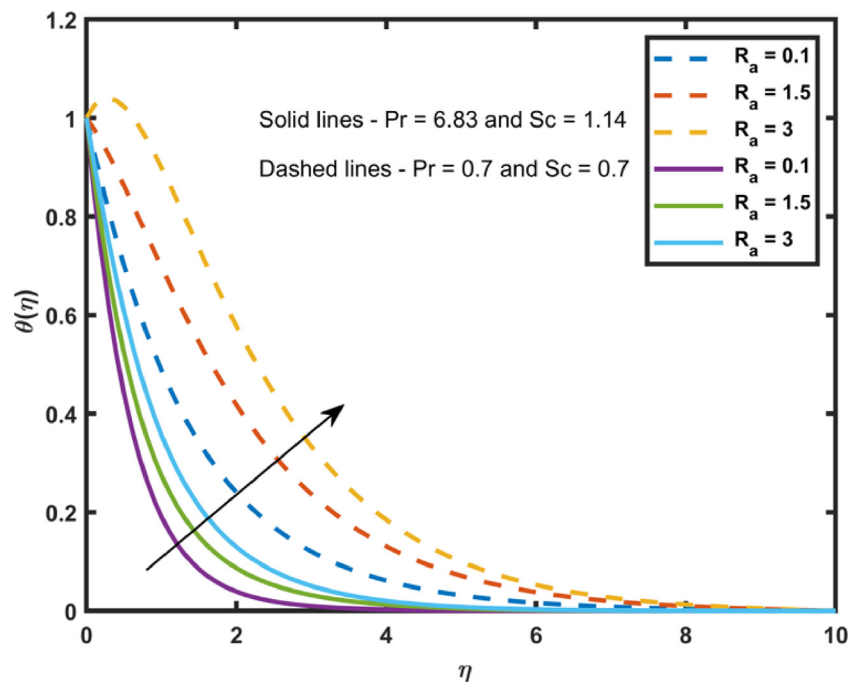


Fig. 17. Temperature distribution for various  $R_a$ .

- It is further seen that, that role of Prandtl number in the temperature distribution is vital, for their effects on radiation absorption are significant.
- In the absence of  $R_a$ , the results are identical to that of Raju et al.<sup>33</sup>

#### Declaration of competing interest

The authors declare that they have no known competing financial interests or personal relationships that could have appeared to influence the work reported in this paper.

#### Data availability

No data was used for the research described in the article

#### Funding

This research did not receive any specific grant from funding agencies in the public, commercial, or not-for-profit sectors.

#### References

- Magyari E, Keller B. Heat and mass transfer in the boundary layers on an exponentially stretching continuous surface. *J Phys D Appl Phys*. 1999;32(5):577–585. <http://dx.doi.org/10.1088/0022-3727/32/5/012>.
- Gupta PS, Gupta AS. Heat and mass transfer on a stretching sheet with suction or blowing. *Can J Chem Eng*. 1977;55(6):744–746. <http://dx.doi.org/10.1002/cjce.5450550619>.
- Elbashareshy EM. Heat transfer over an exponentially stretching continuous surface with suction. *Arch Mech*. 2001;53(6):643–651.
- Al-Odat MQ, Damseh RA, Al-Azab TA. Thermal boundary layer on an exponentially stretching continuous surface in the presence of magnetic field effect. *Int J Appl Mech Eng*. 2006;11(2):289–299.
- Kataria HR, A.S. Mittal. Velocity, mass and temperature analysis of gravity-driven convection nanofluid flow past an oscillating vertical plate in the presence of magnetic field in a porous medium. *Appl Therm Eng*. 2017;110:864–874. <http://dx.doi.org/10.1016/j.applthermaleng.2016.08.129>.
- Shamshuddin MD, Mabood F, Rajput GR, Bég OA, Badruddin IA. Thermo-solutal dual stratified convective magnetized fluid flow from an exponentially stretching riga plate sensor surface with morphogenesis. *Int Commun Heat Mass Transfer*. 2022;134:105997. <http://dx.doi.org/10.1016/j.icheatmasstransfer.2022.105997>.
- Sajid M, Hayat T. Influence of thermal radiation on the boundary layer flow due to an exponentially stretching sheet. *Int Commun Heat Mass Transfer*. 2008;35(3):347–356. <http://dx.doi.org/10.1016/j.icheatmasstransfer.2007.08.006>.
- Bidin B, Nazar R. Numerical solution of the boundary layer flow over an exponentially stretching sheet with thermal radiation. *Eur J Sci Res*. 2009;33(4):710–717.
- Ishak A. MHD boundary layer flow due to an exponentially stretching sheet with radiation effect. *Sains Malays*. 2011;40(4):391–395.
- Mandal IC, Mukhopadhyay S. Heat transfer analysis for fluid flow over an exponentially stretching porous sheet with surface heat flux in porous medium. *Ain Shams Eng J*. 2013;4(1):103–110. <http://dx.doi.org/10.1016/j.asej.2012.06.004>.
- Sheikholeslami M, Kataria HR, Mittal AS. Radiation effects on heat transfer of three dimensional nanofluid flow considering thermal interfacial resistance and micro mixing in suspensions. *Chinese J Phys*. 2017;55(6):2254–2272. <http://dx.doi.org/10.1016/j.cjph.2017.09.010>.
- Patel HR, Mittal AS, Darji RR. MHD flow of micropolar nanofluid over a stretching/shrinking sheet considering radiation. *Int Commun Heat Mass Transf*. 2019;108:104322. <http://dx.doi.org/10.1016/j.icheatmasstransfer.2019.104322>.
- Mittal AS, Kataria HR. Three dimensional CuO–water nanofluid flow considering Brownian motion in presence of radiation. *Karabala Int J Mod Sci*. 2018;4(3):275–286. <http://dx.doi.org/10.1016/j.kijoms.2018.05.002>.
- Mittal AS. Analysis of water-based composite MHD fluid flow using HAM. *Int J Ambient Energy*. 2021;42(13):1538–1550. <http://dx.doi.org/10.1080/01430750.2019.1611648>.
- Mittal AS. Study of radiation effects on unsteady 2D MHD Al2O3–water flow through parallel squeezing plates. *Int J Ambient Energy*. 2022;43(1):653–660. <http://dx.doi.org/10.1080/01430750.2019.1662843>.
- Kataria HR, Mittal AS. Mathematical model for velocity and temperature of gravity-driven convective optically thick nanofluid flow past an oscillating vertical plate in presence of magnetic field and radiation. *J Niger Math Soc*. 2015;34(3):303–317. <http://dx.doi.org/10.1016/j.jnms.2015.08.005>.
- Rahman M, Ferdows M, Shamshuddin MD, Koulali A, Eid MR. Aiding (opponent) flow of hybrid copper–aluminum oxide nanofluid towards an exponentially extending (lessening) sheet with thermal radiation and heat source (sink) impact. *J Pet Sci Eng*. 2022;215:110649. <http://dx.doi.org/10.1016/j.petrol.2022.110649>.
- Sheikholeslami M, Kataria HR, Mittal AS. Effect of thermal diffusion and heat-generation on MHD nanofluid flow past an oscillating vertical plate through porous medium. *J Mol Liq*. 2018;257:12–25. <http://dx.doi.org/10.1016/j.molliq.2018.02.079>.
- Shamshuddin MD, Rajput GR, Mishra SR, Salawu SO. Radiative and exponentially space-based thermal generation effects on an inclined hydromagnetic aqueous nanofluid flow past thermal slippage saturated porous media. *Int J Mod Phys B*. 2023;37(21):2350202. <http://dx.doi.org/10.1142/S0217979223502028>.
- Rajput GR, Jadhav BP, Salunkhe SN. Magnetohydrodynamics boundary layer flow and heat transfer in porous medium past an exponentially stretching sheet under the influence of radiation. *Heat Transf*. 2020;49(5):2906–2920. <http://dx.doi.org/10.1002/hjt.21752>.

21. Shamshuddin MD, Khan SU, Bég OA, T.A. Beg. Hall current, viscous and joule heating effects on steady radiative 2-D magneto-power-law polymer dynamics from an exponentially stretching sheet with power-law slip velocity: a numerical study. *Therm Sci Eng Prog.* 2020;20:100732. <http://dx.doi.org/10.1016/j.tsep.2020.100732>.
22. Shamshuddin MD, Salawu SO, Ogunseye HA, Mabood F. Dissipative power-law fluid flow using spectral quasi linearization method over an exponentially stretchable surface with hall current and power-law slip velocity. *Int Commun Heat Mass Transf.* 2020;119:104933. <http://dx.doi.org/10.1016/j.icheatmasstransfer.2020.104933>.
23. Kataria HR, Mistry M, Mittal A. Influence of nonlinear radiation on MHD micropolar fluid flow with viscous dissipation. *Heat Transf.* 2022;51(2):1449–1467. <http://dx.doi.org/10.1002/htj.22359>.
24. Kataria H, Mittal AS, Mistry M. Effect of nonlinear radiation on entropy optimised MHD fluid flow. *Int J Ambient Energy.* 2022;43(1):6909–6918. <http://dx.doi.org/10.1080/01430750.2022.2059000>.
25. Reddy NN, Rao VS, Reddy BR. Chemical reaction impact on MHD natural convection flow through porous medium past an exponentially stretching sheet in presence of heat source/sink and viscous dissipation. *Case Stud Therm Eng.* 2021;25:100879. <http://dx.doi.org/10.1016/j.csite.2021.100879>.
26. Patel H, Mittal A, Nagar T. Fractional order simulation for unsteady MHD nanofluid flow in porous medium with sores and heat generation effects. *Heat Transf.* 2023;52:563–584. <http://dx.doi.org/10.1002/htj.22707>.
27. Shamshuddin MD, Bég OA, Akkurt N, Leonard HJ, Bég TA. Analysis of unsteady thermo-solutal MoS<sub>2</sub>-EO brinkman electro-conductive reactive nanofluid transport in a hybrid rotating hall MHD generator. *Partial Differ Equ Appl Math.* 2023;24:100525. <http://dx.doi.org/10.1016/j.padiff.2023.100525>.
28. Shamshuddin MD, Shahzad F, Jamshed W, Bég OA, Eid MR, Bég TA. Thermo-solutal stratification and chemical reaction effects on radiative magnetized nanofluid flow along an exponentially stretching sensor plate: Computational analysis. *J Magn Magn Mater.* 2023;565:170286. <http://dx.doi.org/10.1016/j.jmmm.2022.170286>.
29. Casson N. A flow equation for the pigment oil suspensions of the printing ink type. In: *Rheology of Disperse Systems*. Mill CC, ed. New York, NY: Pergamon Press; 1959:84–102.
30. Mukhopadhyay S, Vajravelu K, Van Gorder RA. Casson fluid flow and heat transfer at an exponentially stretching permeable surface. *J Appl Mech.* 2013;80(5):054502. <http://dx.doi.org/10.1115/1.4023618>, 9.
31. Pramanik S. Casson fluid flow and heat transfer past an exponentially porous stretching surface in presence of thermal radiation. *Ain Shams Eng J.* 2014;5(1):205–212. <http://dx.doi.org/10.1016/j.asej.2013.05.003>.
32. Mukhopadhyay S, Moindal IC, Hayat T. MHD boundary layer flow of casson fluid passing through an exponentially stretching permeable surface with thermal radiation. *Chin Phys B.* 2014;23(10):104701. <http://dx.doi.org/10.1088/1674-1056/23/10/104701>.
33. Raju CS, Sandeep N, Sugunamma V, Babu MJ, Reddy JR. Heat and mass transfer in magnetohydrodynamic casson fluid over an exponentially permeable stretching surface. *Eng Sci Technol Int J.* 2016;19(1):45–52. <http://dx.doi.org/10.1016/j.jestch.2015.05.010>.
34. Shercliff JA. *A Textbook of Magnetohydrodynamics*. Oxford, UK: Pergamon Press; 1965.
35. Ibrahim FS, Elaiw AM, Bakr AA. Effect of the chemical reaction and radiation absorption on the unsteady MHD free convection flow past a semi infinite vertical permeable moving plate with heat source and suction. *Commun Nonlinear Sci Numer Simul.* 2008;13(6):1056–1066. <http://dx.doi.org/10.1016/j.cnsns.2006.09.007>.
36. Kumar AV, Bhanumathi D, Varma SV, Yadav YR. Effect of the heat source, radiation absorption and chemical reaction on the unsteady MHD free convective flow past an exponentially accelerated vertical moving plate. *Adv Appl Fluid Mech.* 2013;14(2):147–167.
37. Narayana PS, Venkateswarlu B, Venkataramana S. Effects of hall current and radiation absorption on MHD micropolar fluid in a rotating system. *Ain Shams Eng J.* 2013;4(4):843–854. <http://dx.doi.org/10.1016/j.asej.2013.02.002>.
38. Balamurugan KS, Ramaiah P, Varma SVK, Ramaprasad JL. Thermal radiation and radiation absorption effects on unsteady MHD double diffusive free convection flow of kuvshinski fluid past a moving porous plate embedded in a porous medium with chemical reaction and heat generation. *Far East J Math Sci.* 2014;91(2):211–231.
39. Umamaheswar M, Raju MC, Varma SV. MHD convective heat and mass transfer flow of a Newtonian fluid past a vertical porous plate with chemical reaction, radiation absorption and thermal diffusion. *Int J Eng Res Afr.* 2015;19:37–56. <http://dx.doi.org/10.4028/www.scientific.net/JERA.19.37>.
40. Reddy YS, Varma SV, Balamurugan KS, Ramaprasad JL. Chemical reaction and radiation absorption effects on hydromagnetic free convection flow past a vertical plate with constant mass flux. *Far East J Math Sci.* 2015;98(2):133–149.
41. Ajibade AO, Umar AM. Effect of chemical reaction and radiation absorption on the unsteady MHD free convection couette flow in a vertical channel filled with porous materials. *Afr Mat.* 2016;27:201–213. <http://dx.doi.org/10.1007/s13370-015-0334-7>.
42. Sreedevi G, Rao RR, Rao DP, Chamkha AJ. Combined influence of radiation absorption and hall current effects on MHD double-diffusive free convective flow past a stretching sheet. *Ain Shams Eng J.* 2016;7(1):383–397. <http://dx.doi.org/10.1016/j.asej.2015.11.024>.
43. Reddy SH, Raju MC, Reddy EK. Radiation absorption and chemical reaction effects on MHD flow of heat generating casson fluid past oscillating vertical porous plate. *Front Heat Mass Transf.* 2016;7(1):21. 9.
44. Brewster MQ. *Thermal Radiative Transfer and Properties*. New York, NY: John Wiley and Sons; 1992.
45. Kierzenka J, Shampine LF. A BVP solver based on residual control and the Matlab PSE. *ACM Trans Math Software.* 2001;27(3):299–316.
46. Shampine LF, Gladwell I, Thompson S. *Solving ODEs with MATLAB*. Cambridge: Cambridge University Press; 2003. <http://dx.doi.org/10.1017/cbo9780511615542>.
47. Kierzenka J. Tutorial on solving BVPs with BVP4c. MATLAB central file exchange. 2023 Accessed 15 May 2023. <https://www.mathworks.com/matlabcentral/fileexchange/3819-tutorial-on-solving-bvps-with-bvp4c>.
48. Keskin AÜ. Chapter 10: Solution of BVPs using bvp4c and bvp5c of MATLAB. In: *Boundary Value Problems for Engineers with MATLAB Solutions*. Cham, Switzerland: Springer; 2009. [http://dx.doi.org/10.1007/978-3-030-21080-9\\_10](http://dx.doi.org/10.1007/978-3-030-21080-9_10).